Journal of Soft Computing Paradigm (ISSN: 2582-2640)
www.irojournals.com/jscp/

White Blood Cell Segmentation and Determination of Nucleus to Cytoplasm Ratio by using Microscopic Images

Kirubakaran J.[1], Harikrishna G.[2], Rajesh G.[3], Hemanth V.[4]

[1]Associate Professor, [2-4]U.G. Students, Muthayammal Engineering College, Rasipuram, India

E-mail: 'Kirubakaranj.rnd2@gmail.com, [2]gunjiharikrishna0987@gmail.com, 'rajesjgunapati95@gmail.com, 'vayalahemanth@gmail.com

Abstract

This work utilizes a U-Net convolutional neural network for the segmentation of white blood cell (WBC) components, specifically targeting the nucleus and cytoplasm. This work utilizes a U-Net convolutional neural network for the segmentation of white blood cell (WBC) components, specifically targeting the nucleus and cytoplasm. Accurate WBC segmentation is challenging due to differences in cell shape, size, and staining quality. The segmented regions are further used to compute the cytoplasm-to-nucleus (C/N) ratio, which plays a vital role in medical diagnostics. Input images are pre-processed through normalization and resized to a standard dimension of 256 × 256 pixels. Batch normalization is applied to enhance model stability and convergence. The model is trained and deployed using Google Colab, achieving an accuracy of 80%. The proposed framework provides an effective solution for automated analysis of WBC images.

Keywords: Cytoplasm, Nucleus. Batch Normalization, U-Net, WBC.

DOI: https://doi.org/10.36548/jscp.2025.2.001
Received: 16.03.2025, received in revised form: 14.04.2025, accepted: 30.04.2025, published: 09.05.2025

1. Introduction

The motivation for employing a U-Net convolutional neural network (CNN) for segmenting white blood cell (WBC) components, specifically the nucleus and cytoplasm, and computing the cytoplasm-to-nucleus (C/N) ratio stems from the vital role this ratio plays in medical diagnostics. Variations in the C/N ratio can indicate pathological conditions such as infections, leukemia, and other hematological disorders. Accurate segmentation of these cellular components is essential for identifying morphological anomalies that can signal disease.

U-Net's encoder-decoder architecture with skip connections allows for precise localization and classification of features within an image, making it particularly well-suited for biomedical image segmentation tasks like WBC analysis. Studies have demonstrated that U-Net achieves high accuracy in segmenting nuclei and cytoplasm across various leukocyte types, including lymphocytes, monocytes, neutrophils, eosinophils, and basophils. This precision facilitates the computation of the C/N ratio, aiding in the differentiation between normal and abnormal cells.

Analyzing white blood cell (WBC) images manually is often slow and subject to inconsistencies between observers, which can compromise diagnostic accuracy. To address the existing challenges, the study recommends a U-Net-based deep learning framework designed to accurately segment key WBC components, namely the nucleus and cytoplasm, and determine the cytoplasm-to-nucleus (C/N) ratio, a valuable metric in medical diagnostics. By utilizing automated segmentation, the approach aims to improve the speed and reliability of WBC image analysis. Preprocessing techniques such as image normalization, resizing to a standard 256 × 256 resolution, and batch normalization are applied to enhance model performance and training stability. The model is implemented on Google Colab to ensure accessibility and scalability for practical clinical use. Ultimately, the goal is to create an efficient and accurate tool to support automated WBC evaluation in diagnostic workflows.[1]

2. Literature survey

Khan et al. [2] Introduces a novel approach for classifying white blood cell (WBC) types by combining DL and ML techniques. The authors utilize AlexNet convolutional neural network to extract multi-layer features from WBC images. These features are then fused and

refined using feature selection strategies to enhance their discriminative power. The refined features are subsequently classified using the efficient and fast learning algorithm, an Extreme Learning Machine (ELM),

J. Yao,[3] presents the white blood cells (WBCs) classification using object detection techniques. The authors employ state-of-the-art models, specifically YOLOv4, and Faster R-CNN to simultaneously detect and classify different types of WBCs in microscopic images. This integrated method streamlines the process by combining segmentation and recognition into a single step, enhancing both speed and accuracy.

J. A. et al [4] introduces an approach for automating the WBC classification using a Deep Features based Convolutional Neural Network (DFCNN). A combined CNN architecture integrating AlexNet, GoogLeNet, and ResNet-50 is employed to extract a comprehensive set of features from WBC images. A hybrid algorithm combining the Mayfly Algorithm with Particle Swarm Optimization (HMA-PSO) is utilized to select the most relevant features, enhancing the efficiency and accuracy of the classification model. The selected features are input into an RNN with LSTM to classify WBCs.

Pfeil et al. [5] investigated the application of deep learning in conjunction with mobile microscopy for analyzing blood samples. Their work introduces a portable, point-of-care system that employs an inexpensive mobile microscope, an eyepiece camera, and a smartphone for visualizing human blood. They trained and refined several deep learning models, specifically Mask R-CNN, Mask Scoring R-CNN, D2Det, and YOLACT, for instance, segmentation tasks aimed at identifying and classifying various types of blood cells. Their findings indicated a 93% detection rate of actual blood cells, achieving a mean average precision of 0.57 and a mean average recall of 0.61.

Ashish Girdhar et al. [6] presents an innovative approach to automating the WBC classification. The authors propose a deep learning model utilizing CNN to accurately identify and classify different WBCs, such as lymphocytes, neutrophils, eosinophils, basophils, and monocytes, from peripheral blood smear images. The model was trained as well as evaluated using publicly available datasets, achieving a high classification accuracy of 98.55%.

Q. Zhai et al. [7] presents an innovative approach to automating the classification of WBCs using whole-slide images (WSIs). The algorithm employs threshold segmentation to quickly locate potential WBC regions within raw WSIs. Subsequently, a deeply aggregated

convolutional neural network (CNN) model processes these segmented regions to classify the WBCs accurately. The aggregation of convolutional features from different layers enhances the integration of spatial and semantic information, enabling the extraction of fine-grained features that are important for precise classification. The algorithm attains a classification accuracy of approximately 98.43%.

E. Başaran et al. [8] introduces an innovative approach that prioritizes both accuracy and interpretability. The proposed framework integrates a lightweight CNN, SqueezeNet, with the interpretability tool LIME. Furthermore, the Minimum Redundancy Maximum Relevance (mRMR) method is employed for feature selection to ensure a balance between the relevance and independence of the chosen features. Finally, a Support Vector Machine (SVM) classifier is used to perform the WBC classification.

Bagido et al [9] presents a deep learning-based approach to classify different types of white blood cells (WBCs) from microscopic images. The authors utilized transfer learning techniques with pre-trained models to enhance classification accuracy. Among the models tested, Inception-ResNetV2 achieved the highest performance, attaining a classification accuracy of 98.4% for a dataset comprising four WBC types.

Cengil, et al. [10] presents a hybrid methodology for WBCs into four types. The study employs two distinct transfer learning strategies: the first involves fine-tuning pre-trained models, AlexNet, ResNet18, and GoogLeNet, using a Kaggle dataset and classifying with softmax and Support Vector Machine (SVM) methods, achieving an accuracy of 99.83% with the ResNet18-SVM combination. The second approach utilizes these models as feature extractors, applying various classifiers and dimensionality reduction techniques like Principal Component Analysis (PCA), resulting in an overall classification accuracy of 97.95%. This research emphasizes the efficacy of combining transfer learning with traditional machine learning techniques for accurate and efficient WBC classification M. Makem et al [11] presents a method for segmenting white blood cell (WBC) nuclei in peripheral blood smear images. This segmentation is essential for automated blood analysis, aiding in the diagnosis of various haematological disorders.

N. Alofi et al. [12] introduces a series of CNN based models for classifying WBC In this work the fine-tuned VGG-16 model achieved the highest classification accuracy of 99.81%**.** This study developed four hybrid models for classification tasks, combining the feature learning

capabilities of CNNs with the discriminative power of traditional machine learning classifiers. Specifically, VGG-16 and MobileNet were used as feature extractors, and Support Vector Machines (SVM) and Quadratic Discriminant Analysis (QDA) were used for the final classification. The VGG-16+SVM model demonstrated the highest accuracy at 98.44%, closely followed by the MobileNet+SVM model with an accuracy of 98.19%.

The inference from the survey reveals a clear advancement in the automation of white blood cell (WBC) classification through deep learning and hybrid models. Pre-trained CNN architectures, such as AlexNet, ResNet, VGG-16, and Inception-ResNetV2, serve as powerful feature extractors, while their integration with machine learning classifiers like SVM, ELM, and RNN-LSTM significantly enhances classification accuracy. Techniques like feature fusion, optimization algorithms (e.g., HMA-PSO, mRMR), and interpretability tools (e.g., LIME) contribute to building robust and explainable models. The highest reported accuracy (99.83%) demonstrates the maturity and effectiveness of these approaches, emphasizing their potential for real-world clinical applications in hematological diagnostics.

3. Methodology

In this work the White Blood Cells Dataset available on Kaggle is used [15]. This dataset comprises a collection of labeled microscopic images representing four major types of white blood cells (WBCs). The dataset includes 212 images of Basophils, 744 of Eosinophils, 561 of Monocytes, and 6,231 of Neutrophils.

The process begins with collecting input images of white blood cells (WBCs), which are then standardized through pre-processing steps. These include resizing all images to 256 × 256 pixels to ensure consistency and applying batch normalization to stabilize and accelerate the training of the neural network. Following pre-processing, the images undergo segmentation using a U-Net model, a deep learning architecture well-suited for biomedical image analysis. The U-Net effectively isolates key components of the WBCs, specifically the nucleolus and cytoplasm, by generating precise segmentation masks. Finally, the cytoplasm-to-nucleolus (C/N) ratio is calculated by measuring the segmented areas of the cytoplasm and nucleolus. This ratio serves as an important diagnostic metric in identifying abnormal WBC morphology, aiding in the detection of various hematological conditions. Figure 1 shows the proposed block diagram.[13]

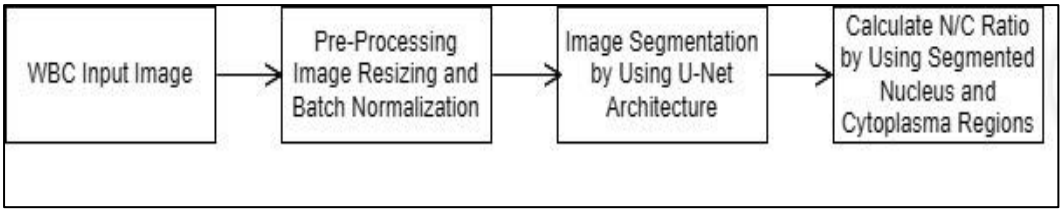

Figure 1. Proposed Block Diagram of WBC Image Segmentation

The image segmentation task for white blood cell (WBC) analysis is handled using a custom U-Net architecture, a convolutional neural network specifically customized for biomedical image segmentation. The U-Net backbone is designed with a symmetric structure comprising an encoder **(**downsampling path**)** and a decoder (upsampling path**)**, which allows for efficient feature extraction and accurate localization. The model includes standard deep learning layers such as convolutional layers for feature extraction, batch normalization to stabilize and speed up training, ReLU activations for non-linearity, max pooling for downsampling, and upsampling layers to reconstruct the segmented output at the original resolution.

The U-Net architecture used in this work, follows the standard encoder-decoder structure with skip connections, which enables precise localization by combining high-resolution features from the contracting path with contextual information from the expansive path. The encoder consists of a series of convolutional blocks, each containing two convolutional layers with a kernel size of 3 × 3, followed by a rectified linear unit (ReLU) activation and a 2 × 2 max-pooling operation for downsampling. The number of filters doubles at each downsampling step, typically starting from 64 and increasing to 128, 256, 512, and up to 1024 in the bottleneck layer.

Within the decoder, the upsampling process involves iterative steps. Each step starts by increasing the spatial dimensions of the feature map using a 2 × 2 transposed convolution(up-convolution). To retain fine-grained details, the upsampled feature map is then concatenated with the corresponding high-resolution feature map from the encoder through skip connections. These combined features are further refined by two consecutive 3 × 3 convolutional layers with ReLU activation. The number of feature channels is progressively reduced by half at each upsampling stage, mirroring the encoder's contraction. The final output layer utilizes a 1 × 1 convolution to produce a feature map with the desired number of classes (nucleus and cytoplasm), followed by a softmax activation depending on the segmentation strategy.

Batch normalization is applied after each convolutional layer to stabilize learning and accelerate convergence. This architecture enables the model to learn both global context and fine-grained details, making it well-suited for biomedical image segmentation tasks like WBC component analysis.

The dataset was divided into three subsets for training, validation, and testing purposes, with a split ratio of 70%, 15%, and 15%, respectively. To enhance the model's ability to generalize to unseen data, data augmentation techniques, including rotations, flips, zoom operations, and brightness modifications, were applied to the training set. The model was trained using the Adam optimization algorithm with an initial learning rate of 0.001 and a batch size of 16. The binary cross-entropy function was used to calculate the loss during training. Early stopping and learning rate scheduling were used to optimize training. The framework was implemented on Google Colab with GPU support. Binary focal loss was used to handle class imbalance by focusing more on hard-to-segment regions like the nucleus and cytoplasm, improving accuracy in detecting smaller structures.

3.1 Training Details

The model is trained using the Adam optimizer with a learning rate of 0.0004 ensuring adaptive learning during training. For the loss function, binary focal loss (with gamma = 2) is employed to address class imbalance and focus more on difficult-to-classify pixels. The training was conducted for 60 epochs using a dataset comprising 50 paired samples of WBC images and their corresponding segmentation masks. A separate set of unseen blood cell images was used for testing to evaluate the model’s generalization capabilities.[14]

The pre-processing pipeline included several important steps:

- Image resizing to 256 × 256 pixels to ensure uniform input size.
- Normalization by scaling pixel values to standardize intensity.
- Grayscale conversion, simplifying the image structure and reducing computational complexity

3.2 Model Performance

To determine the model's performance, the Jaccard Coefficient (Intersection over Union) was used as the primary metric. The model achieved an accuracy of 80% on the test set,

indicating reliable performance in segmenting the nucleolus and cytoplasm of WBCs. Despite a moderately high final loss of 1.2**,** the model demonstrates robustness in WBC image segmentation tasks with limited data.

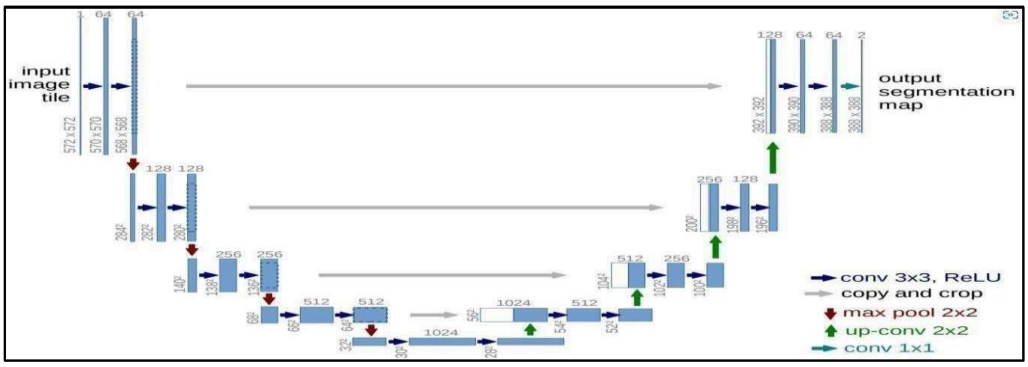

Figure 2. U-Net Architecture [16]

The U-Net architecture (Figure 2) consists of four main stages. The Contracting Path (Encoder) captures image context using repeated 3×3 convolutions followed by ReLU and 2×2 max pooling, doubling feature channels from 64 to 1024. The Bottleneck connects encoder and decoder with two 3×3 convolutions and an up-convolution, reducing channels from 1024 to 512. The Expanding Path (Decoder) upsamples the features using transposed convolutions, concatenates with encoder features (skip connections), and applies two 3×3 convolutions, gradually reducing channels from 512 to 64. Finally, the Output Layer uses a 1×1 convolution to map the features to the desired number of classes for segmentation. In this work, the Categorical Cross-Entropy (CCE) loss function is sufficient for handling the two-level segmentation task involving both the nucleus and cytoplasm. [14]

4. Result and Discussion

Figure 3(a) shows the WBC input image of a neutrophil, while Figures 3(b) and 3(c) depict the segmented nucleus and cytoplasm regions of the neutrophil using the U-Net architecture. Figure 4(a) displays the WBC input image of an eosinophil, and Figures 4(b) and 4(c) show the segmented nucleus and cytoplasm regions of the eosinophil using U-Net. Figure 5(a) presents the WBC input image of a basophil, with Figures 5(b) and 5(c) illustrating the segmented nucleus and cytoplasm regions of the basophil using U-Net. Finally, Figure 6(a) shows the WBC input image of a monocyte, and Figures 6(b) and 6(c) display the segmented nucleus and cytoplasm regions of the monocyte using the U-Net architecture.

(a) Input Image (b) Nucleus of WBC (c) Cytoplasm of WBC

Figure 3. Neutrophil

(a) Input Image **(b)** Nucleus of WBC (c) Cytoplasm of WBC

Figure 4. Eosinophil

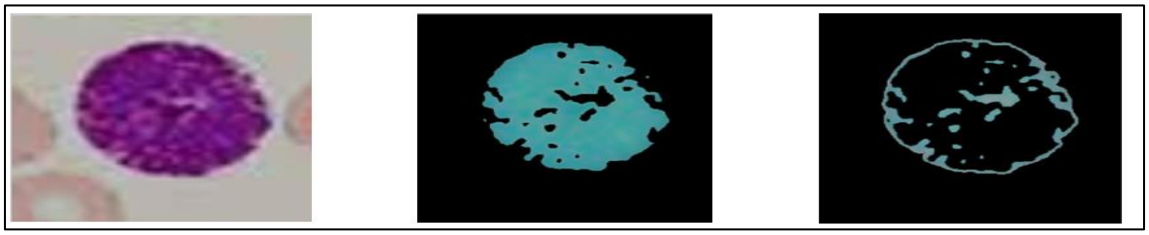

(a) Input Image **(b)** Nucleus of WBC (c) Cytoplasm of WBC

Figure 5. Basophil

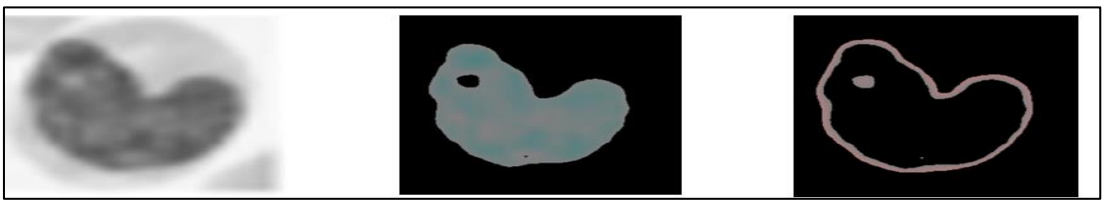

(a) Input Ima **(b)** Nucleus of WBC (c) Cytoplasm of WBC

Figure 6. Monocyte

4 .1 Determination of Nucleus- Cytoplasm Ratio of WBC Analysis.

The inference from the Table 1 analysis of neutrophil images based on the nucleus-to-cytoplasm (N/C) pixel ratio. The healthy neutrophils typically exhibit N/C pixel ratios and mean ratios close to 1, reflecting a balanced proportion between nucleus and cytoplasm. In contrast, unhealthy neutrophils show significantly higher N/C ratios (greater than 1.5), suggesting an enlarged nucleus or reduced cytoplasm, features commonly associated with abnormal or pathological conditions. These observations highlight that the N/C ratio, both in terms of pixel count and mean intensity, serves as a reliable indicator for identifying potential abnormalities in neutrophil morphology.

Table 1. Neutrophil (the Nucleus-Cytoplasm Ratio with Respect to their Pixel Values and Ratio of Mean)

Figure No.	No. of pixels(N)	No. of pixel (C)	N/C Ratio(P)	Mean	Mean	N/C ratio(m)	Result
	Nucleus	cytoplasm		Nucleus	Cytoplasm		
1	10164	10606	0.9583	14.0528	15.7522	0.9125	Healthy
2	15896	18032	0.8816	33.0139	39.2641	0.8448	Healthy
3	14870	13819	1.0759	31.3286	30.8258	1.015	Healthy
4	12077	15598	0.7744	22.336	31.2474	0.7236	U.H
5	11879	7798	1.5226	25.6625	17.1831	1.4663	UH
6	15896	19032	0.8353	35.9927	41.8241	0.8638	Healthy
7	18078	8778	2.0582	28.9141	14.322	1.9523	UH
8	11239	4996	2.2471	22.5486	10.2096	2.1107	UH
9	12366	10660	1.1598	22.903	18.6996	1.2133	Healthy
10	6824	3356	2.0303	14.6884	7.322	1.8851	UH
11	13334	14620	0.9121	28.6628	30.4773	0.9423	Healthy

The observed from the Table 2 eosinophil analysis. The healthy cells generally have higher N/C pixel ratios (around 1.8–2.0) and corresponding mean ratios, indicating a prominent nucleus. Unhealthy cells tend to have lower ratios, suggesting morphological abnormalities.

Table 2. Eosinophil- Nucleus- Cytoplasm Ratio with Respect to their Pixel Values and Ratio of Mean.

Figure No.	No. of pixels(N)	No. of pixel (C)	N/C Ratio(P)	Mean	Mean	N/C ratio(m)	Result
	Nucleus	Cytoplasm		Nucleus	Cytoplasm		
12	6824	3356	2.0301	13.6884	6.3224	1.8850	Healthy
13	12509	6595	1.8956	24.9142	11.7521	1.9570	healthy
14	12014	6525	1.8399	25.4213	12.4103	1.9028	Healthy
15	12183	13180	0.9244	26.2351	26.1432	1.0032	U,H.
16	14127	7550	1.8699	23.7333	12.0765	1.8281	Healthy
17	13334	14629	0.9115	27.6628	29.4773	0.9423	UH
18	14706	23671	0.6214	26.2887	43.7175	0.6187	UH
19	16776	11127	1,5072	27.8983	17.3793	1.5263	UH
20	17681	22707	0.7787	21.903	17.6996	1.2133	UH
21	15770	27061	0.5829	25.3058	47.4806	0.5518	Healthy*

The analysis of Table 3 shows basophils reveals that most healthy cells exhibit high N/C pixel ratios (around 3.5 to 5.0) and similarly elevated mean ratios, indicating a nucleus-dominant structure typical for basophils. Unhealthy cases show either extremely high or inconsistent ratios, suggesting morphological irregularities. Overall, both pixel and mean ratios effectively distinguish healthy from abnormal basophils

Table 3. Basophil - Nucleus- Cytoplasm Ratio with Respect to their Pixel Values and Ratio of Mean

Figure No.	No. of pixels(N)	No. of pixel (C)	N/C Ratio(P)	Mean	Mean	N/C ratio(m)	Result
	Nucleus	cytoplasm		Nucleus	Cytoplasm		
22	26223	4304	6,080	17.4164	3.8483	3.3200	U.H
23	16204	4076	3.9681	10.4491	1.5337	3.5306	Healthy
24	28448	8337	3.5093	59.2961	13.7867	3.8827	Healthy
25	24736	5636	4.3829	50.1382	11.0224	4.0037	healt

							hy
26	30517	6067	5.0233	50.3833	8.9865	4.7676	healthy
27	26920	5064	5.3074	36.0445	8.0706	3.7777	UH
28	26894	10867	2.4734	56.9717	22.9517	2.3634	UH
29	32711	6576	4.9682	59.4263	11.1142	4.6839	Healthy
30	40832	8661	4.7101	76.3398	15.5815	4.4557	Healthy
31	35456	7039	5.0313	54.9406	10.6219	4.5112	Healthy

Table 4 shows that healthy monocytes have a higher nucleus-to-cytoplasm (N/C) pixel ratio and a higher mean intensity ratio, typically with N/C values above 3.0 and mean ratios above 3.0. In contrast, unhealthy (UH) monocytes display lower N/C ratios (around or below 2.0) and more balanced or higher cytoplasm intensities. Thus, both pixel and intensity-based N/C ratios effectively distinguish healthy from unhealthy monocytes. The results were obtained using the figures collected from White Blood Cells Dataset [15].

Table 4. Monocyte - Nucleus- Cytoplasm Ratio with Respect to their Pixel Values and Ratio of Mean

Fig No.	No. of pixels(N)	No. of pixel (C)	N/C Ratio(P)	Mean	Mean	N/C ratio(m)	Result
	Nucleus	cytoplasm		Nucleus	Cytoplasm		
32	19666	4628	4.2423	29.775	0.2732	3.8717	Healthy
33	19724	5454	3.6116	47.8477	2.8916	4.4872	Healthy
34	22835	6423	3.5512	40.6659	3.693	3.7001	Healthy
35	24820	6178	4.0012	49.179	1.8593	5.0512	UH
36	27628	6649	4.1504	42.9046	4.9731	3.5333	Healt

							hy
37	25090	6718	3.9401	42.3982	5.6802	3.7070	Healthy
38	14511	13210	1.0984	14.1973	14.98	0.9686	UH
39	23332	8982	2.5958	46.134	35.669	1.2291	UH
40	11063	8982	1.3044	10.9215	6.3926	1.2767	UH
41	18668	6095	3.0288	26.6628	2.369	3.0152	Healthy

4.2 U-Net Model Training and Validation Graph

Figure 7 shows the training and validation graph of U-Net. From the figure, it is observed that the number of iterations increases, and the validation accuracy maintains stable position. The x-axis indicates number of iterations and y-axis indicates an accuracy of the plot.

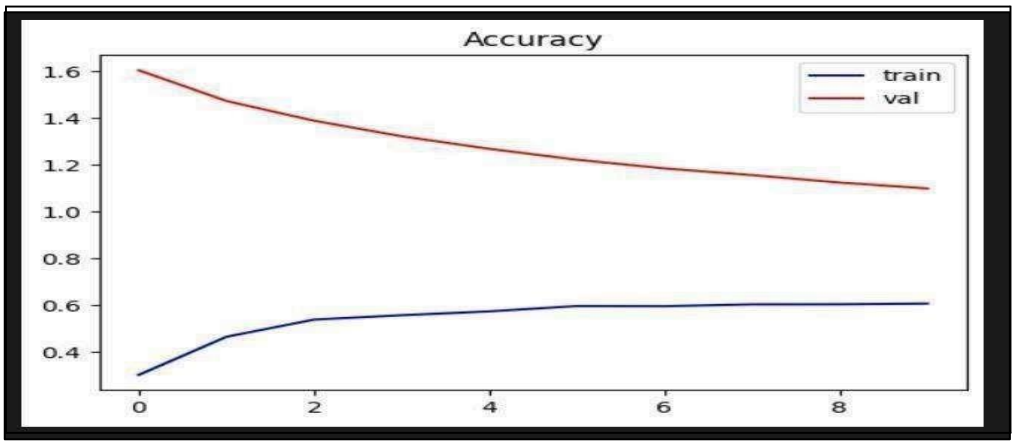

Figure 7. Training and Validation Graph

5. Conclusion

The segmentation of white blood cells was performed using the U-Net architecture, incorporating preprocessing steps such as resizing images to 256×256 pixels and applying batch normalization to enhance model stability and performance. The model, trained and evaluated on Google Colab, achieved an accuracy of 80%. Following segmentation, the cytoplasm-to-nucleus (C/N) ratio was analyzed across different WBC types,Neutrophils, Eosinophils, Basophils, and Monocytes—to assess structural differences relevant to identifying abnormal

cells. The N/C ratio is a clinically valuable indicator, with elevated values often linked to malignancies like leukemia. This automated approach enables more reliable and consistent early diagnosis by minimizing human error and inter-observer variability.

References

[1] Mohapatra, Subrajeet, Dipti Patra, and Sanghamitra Satpathi. "Image analysis of blood microscopic images for acute leukemia detection." In 2010 international conference on industrial electronics, control and robotics, 215-219. IEEE, 2010.

[2] Khan, Altaf, Amber Eker, Alexander Chefranov, and Hasan Demirel. "White blood cell type identification using multi-layer convolutional features with an extreme-learning machine." Biomedical Signal Processing and Control 69 (2021): 102932.

[3] J Yao, Xiwei Huang, Maoyu Wei, and Lingling Sun., High-efficiency classification of white blood cells based on object detection. Journal of Healthcare Engineering, 2021, Vol. 2021: Article id 1615192.

[4] A. Meenakshi, J. A. Ruth, V. R. Kanagavalli, and R. Uma, Automatic classification of white blood cells using deep features based convolutional neural network. Multimedia Tools and Applications, 2022, Vol.81, 30121-30142.

[5] J. Pfeil, A. Nechyporenko, M. Frohme, Frank T. Hufert and Katja Schulze. Examination of blood samples using deep learning and mobile microscopy. BMC Bioinformatics, 2022, Vol. 23(1), Article 65.

[6] Girdhar, Ashish, Himani Kapur, and Vijay Kumar. "Classification of white blood cell using convolution neural network." Biomedical Signal Processing and Control 71 (2022): 103156.

[7] Q. Zhai, B. Fan, B. Zhang, et a1. Automatic white blood cell classification based on whole-slide images with a deeply aggregated neural network. Journal of Medical and Biological Engineering, 2022, Vol.42, 126-137.

[8] E. Başaran. Classification of white blood cells with SVM by selecting SqueezeNet and LIME properties by mRMR method. Signal, Image and Video Processing, 2022, Vol.16, 1821-1829.

[9] R.A. Bagido, M. Alzahrani, and M. Arif. White blood cell types classification using deep learning models. International Journal of Computer Science & Network Security, 2021, Vol.21(9), 223—229.

[10] Cengil, Emine, Ahmet Çınar, and Muhammed Yıldırım. "A hybrid approach for efficient multi-classification of white blood cells based on transfer learning techniques and traditional machine learning methods." Concurrency and Computation: Practice and Experience 34, no. 6 (2022): e6756.

[11] M. Makem, A. Tiedeu, G. Kom and Yannick Pascal Kamdeu Nkandeu A robust algorithm for white blood cell nuclei segmentation. Multimedia Tools and Applications, 2022, Vol.81(13), 17849-17874.

[12] N. Alofi, W. Alonezi, W. Alawad. WBC-CNN: EfFicient CNN-based models to classify white blood cells subtypes. International Journal of Online & Biomedical Engineering, 2021, Vol. 17(13), 135-150.

[13] G. Sriram, T. R. Ganesh Babu, R. Praveena, and J. V. Anand, (2022) 'Classification of Leukemiaand Leukemoid Using VGG-16 Convolutional Neural Network Architecture' Molecular & Cellular Biomechanics, Vol.19 (1}, 29-40.

[14] S Sasikala, S.Sureshkannan, S Elango, Sundara Rajulu Navaneethakrishnan, R Praveena & T R Ganesh Babu (2024) "Enhancing White Blood Cell Detection in Microscopic Images Through Segmentation and Fusion Methodologies" Proceedings of the Nineth International Conference on Communication and Electronics Systems (ICCES-2024) IEEE Xplore Part Number: CFP24AWO-ART; ISBN: 979-8-3503-7797-2,1118-1123.

[15] https://www.kaggle.com/datasets/masoudnickparvar/white-blood-cells-dataset.

[16] https://github.com/zenetio/U-Net_model/blob/master/README.md.